The EMBO Journal Vol. 20 No. 12 pp. 3210–3217, 2001

The McrBC restriction endonuclease assembles into a ring structure in the presence of G nucleotides

Daniel Panne, Shirley A.Müller[1], Sabine Wirtz[1], Andreas Engel[1] and Thomas A.Bickle[2]

Department of Microbiology and [1]Maurice E.Müller Institute for Structural Biology, Biozentrum, Basel University, Klingelbergstrasse 70, CH-4056 Basel, Switzerland

[2]Corresponding author
e-mail: thomas-a.bickle@unibas.ch

McrBC from *Escherichia coli* K-12 is a restriction enzyme that belongs to the family of AAA$^+$ proteins and cuts DNA containing modified cytosines. Two proteins are expressed from the *mcrB* gene: a full-length version, McrB$_L$, and a short version, McrB$_S$. McrB$_L$ binds specifically to the methylated recognition site and is, therefore, the DNA-binding moiety of the McrBC endonuclease. McrB$_S$ is devoid of DNA-binding activity. We observed that the quaternary structure of the endonuclease depends on binding of the cofactors. In gel filtration experiments, McrB$_L$ and McrB$_S$ form high molecular weight oligomers in the presence of Mg^{2+} and GTP, GDP or GTP-γ-S. Oligomerization did not require the presence of DNA and was independent of GTP hydrolysis. Electron micrographs of negatively stained McrB$_L$ and McrB$_S$ revealed ring-shaped particles with a central channel. Mass analysis by scanning transmission electron microscopy indicates that McrB$_L$ and McrB$_S$ form single heptameric rings as well as tetradecamers. In the presence of McrC, a subunit that is essential for DNA cleavage, the tetradecameric species was the major form of the endonuclease.

Keywords: AAA$^+$ protein family/GTP/GTPase/McrBC restriction/scanning transmission electron microscopy

Introduction

Restriction–modification systems allow bacteria to detect and destroy foreign DNA, thus providing an efficient defense against bacteriophages. This phenomenon was first described in the early 1950s (Luria and Human, 1952; Bertani and Weigle, 1953). The molecular event underlying restriction was later shown to be cleavage of the phage DNA by endonucleases, and the modification was shown to be due to methylation of the DNA (Dussoix and Arber, 1962; Arber, 1965). In the classical restriction–modification systems, DNA modification and restriction work in concert to protect endogenous DNA and exclude exogenous DNA. A restriction endonuclease recognizes a specific DNA sequence and cleaves it if it is not modified. The associated DNA methyltransferase recognizes the same sequence and methylates a key residue within that sequence, thereby preventing cleavage of the host DNA by its own restriction enzyme(s) (Bickle and Krüger, 1993; Roberts and Macelis, 1993).

A fundamentally different way to distinguish between exogenous and endogenous DNA is to recognize a foreign modification pattern. This is accomplished by modification-dependent restriction systems. In this case, the host cell DNA avoids being cleaved because it is not modified. The modification-dependent restriction systems are, therefore, not associated with a methyltransferase (reviewed by Raleigh and Wilson, 1986; Bickle and Krüger, 1993). In fact, the first description of restriction–modification by Luria and Human (1952) is now known to be due to modification-dependent restriction (Revel, 1983).

In *Escherichia coli* K-12 there are at least four chromosomally encoded restriction activities. One, *Eco*KI, is a classical type I restriction–modification system that restricts unmodified DNA. The other three systems, *mcrA*, *mrr* and *mcrBC*, restrict DNA that is methylated at specific sequences (reviewed by Raleigh, 1992; Bickle and Krüger, 1993). McrBC is the best characterized of these methylation-dependent restriction enzymes. The *mcrBC* operon contains two genes, *mcrB* and *mcrC*. The *mcrB* gene shares sequence similarity with members of the AAA$^+$ family of proteins (Neuwald *et al*., 1999). The key feature of the AAA$^+$ family (AAA$^+$ standing for ATPases associated with various cellular activities) is a conserved module of 230–250 amino acids that includes the Walker A and B motifs and other unique regions of similarity (reviewed by Patel and Latterich, 1998). Several *mcrB*-like genes have been identified based on sequence similarity to genes in different microorganisms. These form a subfamily among the large AAA$^+$ family of proteins (Neuwald *et al*., 1999). The AAA$^+$ domain is found in a wide variety of proteins that often perform chaperone-like functions that assist in the assembly, operation or disassembly of protein complexes. For example, the AAA$^+$ domain is found in proteases such as the 19S cap complex of the eukaryotic 26S proteasome and the bacterial FtsH, as well as in the regulatory components of the Lon, Clp and HslVU proteases (Neuwald *et al*., 1999). The AAA$^+$ domain is also associated with protein–DNA complexes; for example, it occurs in proteins involved in replication (DnaA and DnaB) and recombination (RuvB) (Neuwald *et al*., 1999). Frequently proteins that belong to the AAA$^+$ family form hexameric or heptameric ring structures (Pamnani *et al*., 1997; Rohrwild *et al*., 1997; Wolf *et al*., 1998) and it has been proposed that they act as ATP-dependent protein clamps (Confalonieri and Duguet, 1995).

The *mcrB* gene encodes a large, full-length gene product termed McrB$_L$ of 53 kDa and a small McrB$_S$ protein of 34 kDa (Ross *et al*., 1989b; Dila *et al*., 1990; Krüger *et al*., 1992). McrB$_L$ and McrB$_S$ seem to be expressed at equimolar ratios (Ross and Braymer, 1987;

Dila *et al*., 1990). $McrB_S$ lacks the N-terminal 161 amino acids but retains the C-terminal 287 residues (Ross *et al*., 1989b), which include the AAA^+ domain. $McrB_S$ is produced by internal in-frame translational initiation rather than post-translational processing of the full-length product (Ross *et al*., 1989b; Krüger *et al*., 1992). Its role *in vitro* and *in vivo* seems to be to modulate McrBC activity (Beary *et al*., 1997; Panne *et al*., 1998).

The $McrB_L$ subunit confers specificity to the endonuclease by binding to the methylated recognition site R^mC (Krüger *et al*., 1995; Stewart *et al*., 2000). The DNA-binding domain resides in the N-terminal 161 amino acids; evidence for this includes lack of DNA binding by $McrB_S$ and by a mutant with a missense mutation in the N-terminal region (W49C), and retention of DNA-binding ability by an N-terminal fragment of 190 amino acids (Gast *et al*., 1997; Panne *et al*., 1998, 1999). Therefore, McrBs alone or in the presence of McrC cannot support restriction either *in vivo* (D.Dila and E.A.Raleigh, unpublished results; Beary *et al*., 1997) or *in vitro* (Panne *et al*., 1998). *In vitro*, $McrB_L$, McrC, GTP and Mg^{2+} are required for DNA cleavage (Sutherland *et al*., 1992). The *mcrC* gene directs the synthesis of a 40 kDa *mcrC* gene product (Ross *et al*., 1989a). McrC lacks DNA-binding activity but interacts directly with either $McrB_L$ or $McrB_S$ and stimulates their GTPase activity (Pieper *et al*., 1997; Panne *et al*., 1999; Stewart *et al*., 2000). McrBC is, to our knowledge, the only member of the AAA^+ family that uses GTP rather than ATP as a cofactor.

McrBC recognizes and cleaves DNA containing at least two R^mC sites. These recognition sites can be separated by 40 bp–3 kb (Stewart and Raleigh, 1998). Cleavage occurs ~30 bp from either recognition site, independent of the spacing between the two sites (Stewart and Raleigh, 1998; Panne *et al*., 1999). Recent results support the model that communication between distant recognition sites is accomplished by GTP hydrolysis-driven DNA translocation by the McrBC complex (Panne *et al*., 1999). The stalling of such a translocating complex, either by the convergence of two translocating complexes or by a non-specific physical block such as a DNA-bound protein, can induce DNA cleavage (Panne *et al*., 1999).

Subunit titration experiments suggest that the active McrBC endonuclease contains $McrB_L$ and McrC subunits at a ratio of 3–5:1 (Panne *et al*., 1998). To analyze the subunit stoichiometry of the AAA^+ type McrBC endonuclease further, we have investigated the quaternary structure of $McrB_L$, $McrB_S$ and the complex $McrB_LC$.

Results

Gel filtration experiments

Previous studies have shown that the optimal ratio for DNA cleavage is 3–5 $McrB_L$ per McrC, suggesting that DNA cleavage is accomplished by a multisubunit complex (Panne *et al*., 1998). To investigate the nature of this complex further, we performed gel filtration experiments with $McrB_S$ or $McrB_L$ in the presence and absence of the cofactors and analogs GTP, GDP or GTP-γ-S. As shown in Figure 1A, $McrB_S$ alone eluted at 35.7 kDa, which is close to its predicted mol. wt of 34.6 kDa. When $McrB_S$ was pre-incubated in buffer containing GTP or GDP, the protein eluted in two peaks corresponding to mol. wts of ~52 and 217 kDa, respectively. In the presence of GTP-γ-S, most of the protein eluted with a mol. wt of ~217 kDa, with only a small shoulder remaining at 52 kDa. It is possible that the species eluting at 52 kDa represents an intermediate oligomer such as a dimer (see below). Assembly of the 217 kDa species was stabilized by the presence of the non-hydrolyzable GTP-γ-S. Pre-incubation in the presence of ATP did not lead to oligomerization (see Table I).

Similar elution profiles were obtained in gel filtration experiments with the $McrB_L$ subunit (data not shown). In the absence of nucleotide cofactor, the protein eluted as a monomer with a mol. wt of 53 kDa and a very small shoulder at 78 kDa. The size of the major peak was close to the calculated mol. wt of 53.1 kDa. After pre-incubation in the presence of GTP, GDP or GTP-γ-S, the protein eluted with a mol. wt of 344 and 78 kDa (Table II). The species eluting at 344 kDa was predominant in the presence of the non-hydrolyzable GTP-γ-S, whereas, in the presence of GTP or GDP, significant amounts of the 78 kDa intermediate were observed.

Because McrC stimulates GTP hydrolysis by $McrB_L$ and $McrB_S$ and is required for DNA cleavage (Pieper *et al*., 1997; Panne *et al*., 1999; Stewart *et al*., 2000), it is predicted that McrC interacts directly with these McrB subunits. When McrC and $McrB_S$ were pre-mixed in the presence of GTP-γ-S and applied to the gel filtration column, a single peak corresponding to a mol. wt of 505 kDa was observed (Figure 1B). In the presence of GTP or GDP, protein eluted in two peaks with mol. wts of 52 and 505 kDa. In the absence of nucleotide cofactor, $McrB_S$ eluted at its predicted mol. wt of 36 kDa (Table I). For $McrB_L$, a high molecular weight species of 736 kDa was obtained if McrC and GTP-γ-S were present (Table II). The peak eluting at 736 kDa showed $McrB_LC$ endonuclease activity if the reaction mixture was supplemented with 1 mM GTP (data not shown). Assembly of the oligomers was dynamic in that re-injection into the column in the absence of nucleotide cofactor led to dissociation, with $McrB_L$ or $McrB_S$ migrating as monomers (data not shown).

From these results, we conclude that the formation of McrB oligomers is GTP dependent. Oligomerization did not require the presence of DNA and was independent of GTP hydrolysis.

Electron microscopy of McrB oligomers

To understand further the nature of the enzyme oligomers, we analyzed $McrB_S$, $McrB_L$ and $McrB_LC$ samples by scanning transmission electron microscopy (STEM). As shown in Figure 2, images recorded from negatively stained samples containing GTP-γ-S revealed the assembly of $McrB_L$ and $McrB_S$ into 'doughnut'-shaped complexes. The presence of GTP-γ-S was essential for their formation; no such structures were seen in the absence of this nucleotide cofactor (data not shown). Thus, in agreement with the gel filtration experiments, GTP binding but not hydrolysis was found to be essential for $McrB_S$ and $McrB_L$ oligomerization. These 'doughnuts' are considered to be top-view projections (Figure 2A, top rows, and B). The few side-view projections also observed for the $McrB_S$ sample showed that sometimes the two rings are stacked (Figure 2A, bottom row). For the $McrB_L$ sample, the 'doughnut' structure exhibited up to seven

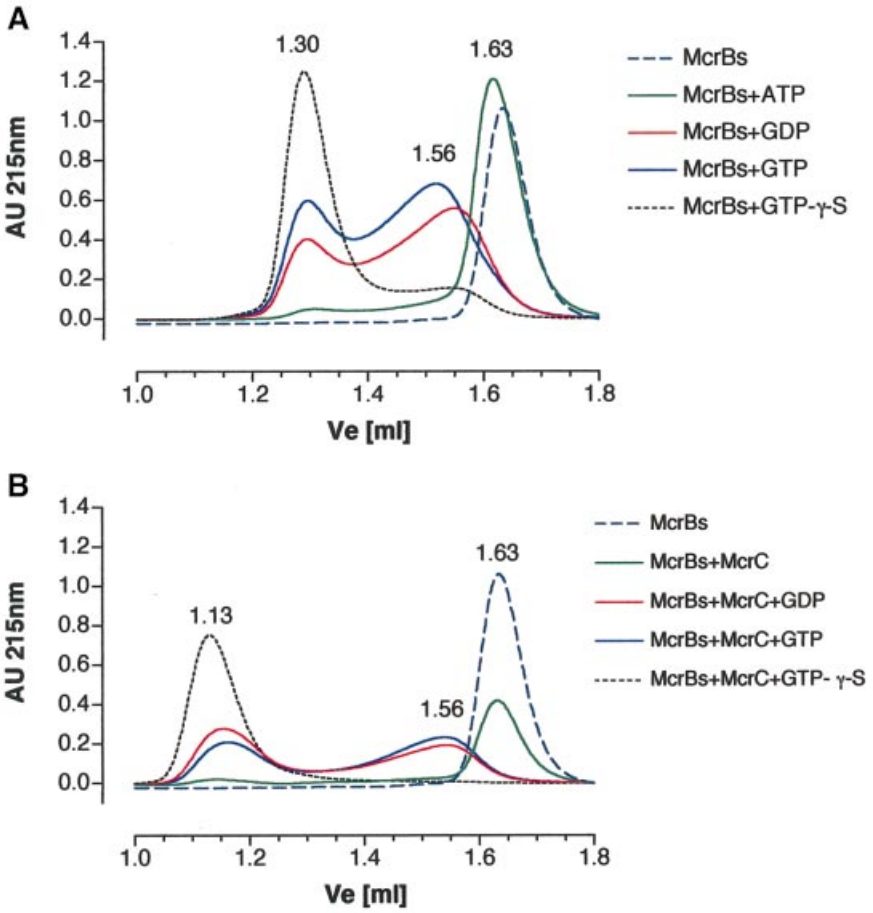

Fig. 1. Gel filtration. (**A**) Elution profile of $McrB_S$ in the presence of the indicated nucleotide cofactors. Without nucleotide cofactor the $McrB_S$ eluted at V_e = 1.63 ml. When 1 mM GTP or GDP was included, two peaks at V_e = 1.30 and 1.56 were observed. Including 1 mM GTP-γ-S shifted almost all of the protein to the V_e = 1.30 peak. In the presence of 1 mM ATP, the protein eluted as a monomer at V_e = 1.62. (**B**) Elution profile in the presence of McrC. An additional peak at V_e = 1.13 was observed.

Table I. Apparent relative masses (kDa) of $McrB_S$ and $McrB_SC$ complexes by gel filtration

Cofactor	$McrB_S$	$McrB_S$ + McrC
None	36	36
GTP	52 and 217	52 and 505
GDP	52 and 217	52 and 505
GTP-γ-S	52 and 217	505
ATP	36	n.d.

n.d., not determined.

Table II. Apparent relative masses (kDa) of $McrB_L$ and $McrB_LC$ complexes by gel filtration

Cofactor	$McrB_L$	$McrB_L$ + McrC
None	52	n.d.
GTP	78 and 344	78 and 736
GDP	78 and 344	78 and 736
GTP-γ-S	78 and 334	736

n.d., not determined.

protrusions (Figure 2B). Such protrusions were observed with different preparations of $McrB_L$. Although their nature remains unclear, it is possible that they correspond to the 19 kDa N-terminal DNA-binding domain, which can exist in different conformations. No protrusions were observed for $McrB_S$, which is missing this N-terminal region. Rotational and translational alignment of negatively stained $McrB_S$ or $McrB_L$ particle projections recorded by conventional transmission electron microscopy did not allow the rotational symmetry, and hence the subunit stoichiometry, for either oligomer to be defined unambiguously (data not shown).

The $McrB_LC$ complex examined was assembled in the presence of GTP-γ-S and purified by gel filtration. Negatively stained particles were visualized by STEM (Figure 2C). Most particles had an elongated shape, representing side views of the endonuclease. The association of two $McrB_L$ oligomers was clearly revealed.

Mass analysis by scanning transmission electron microscopy

To determine the subunit stoichiometry, the masses of freeze-dried, unstained $McrB_S$, $McrB_L$ and $McrB_LC$ oligomers were determined by STEM. The $McrB_S$ and $McrB_L$ samples were prepared by diluting the protein into buffer containing 1 mM GTP-γ-S (see Materials and methods). For the analysis of $McrB_LC$ complexes, $McrB_L$ was pre-mixed with McrC and GTP-γ-S and the resulting

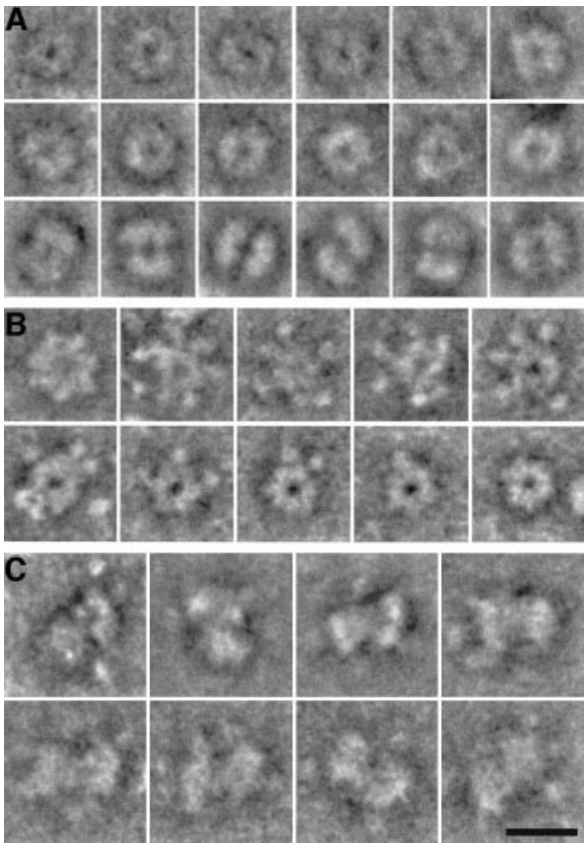

Fig. 2. McrBC complexes formed in the presence of GTP-γ-S. The images were recorded from negatively stained samples by scanning transmission electron microscopy. (**A**) $McrB_S$: the top views shown in the first two rows clearly reveal a ring-shaped structure. Side views of complexes formed from two $McrB_S$ oligomers are displayed in the third row. (**B**) $McrB_L$: up to seven protrusions radiate from the central ring. Distinct side views were not detected on the micrographs. (**C**) $McrB_LC$: the complexes are formed from two $McrB_L$ oligomers. The exact position of McrC cannot be defined. Scale bar, 15 nm.

$McrB_LC$ oligomers were purified by gel filtration. After elution from the column, the $McrB_LC$ sample was supplemented immediately with 1 mM GTP-γ-S and the grid was prepared. The $McrB_LC$ particles were less homogenous when GTP-γ-S was not included after elution of the particles from the gel filtration column (data not shown). In each case, the microscopy grids were washed with quartz double-distilled water and freeze-dried.

Structural details of the complexes could rarely be distinguished on the low dose, dark-field images recorded. For $McrB_S$ and $McrB_L$, the oligomers generally had a circular projection, although a few elongated particles were also observed (Figure 3A and C). In contrast, the $McrB_LC$ complexes mostly had an elongated shape, presumably representing side views of the endonuclease (Figure 3E). In all, 2183 $McrB_S$, 572 $McrB_L$ and 1518 $McrB_LC$ particles were analyzed. The resulting mass histograms are shown in Figure 3 and the masses corresponding to the Gaussian curves fitted are summarized in Table III. For the $McrB_S$ sample, the data fall into two peaks with masses of 239 (± 57) kDa and 468 (± 66) kDa (Figure 3B). As each $McrB_S$ subunit has a mass of 34.6 kDa, the mass of the first peak corresponds well to that of a heptamer, whereas the second peak has a mass close to that of a tetradecamer (Table IV). Similarly, two peaks were obtained for the $McrB_L$ sample with masses of 361 (± 71) kDa and 698 (± 93) kDa (Figure 3D). The $McrB_L$ subunit has a mass of 53.1 kDa and, therefore, the mass of the first peak is again close to that of a heptamer and the mass of the second peak is close to that of a tetradecamer (Table IV). For the $McrB_LC$ complex, there is a single major peak at 759 (± 100) kDa (Figure 3F). The relatively large standard deviation of the measurement reflects protein heterogeneity. This, combined with the 5% absolute calibration uncertainty of the instrument, prohibits the precise definition of the McrC, $McrB_L$ stoichiometry since McrC has a mass of only 40 kDa. Accordingly, the result indicates the association of a $McrB_L$ tetradecamer with one or two molecules of McrC. A small (n ~264) number of particles in this sample were of higher mass, giving rise to the minor mass peak at 994 (± 100) kDa. Only very few particles had masses in the range of $McrB_L$ heptamers. Thus, in agreement with the results obtained by gel filtration, McrC seems to stabilize the association of the two heptameric $McrB_S$ or $McrB_L$ rings.

Discussion

Here we have analyzed the assembly of the methyl-dependent restriction endonuclease McrBC from its constituent subunits. $McrB_L$ and $McrB_S$ both form heptameric ring structures upon incubation with nucleotide cofactor. These heptameric rings can then stack to form tetradecameric cylindrical structures. McrC binding stabilized the tetradecameric form of the endonuclease. These results favor the model that DNA restriction is accomplished by a multisubunit McrBC complex (Panne *et al*., 1998).

Overall, the masses of the particles measured by STEM compare well with those obtained by gel filtration. However, there are some important differences. In the STEM experiments, $McrB_S$ and $McrB_L$ formed tetradecameric as well as heptameric complexes. In the gel filtration experiments, we did not observe the formation of the tetradecameric species in the absence of McrC. Presumably the tetradecamer dissociates during gel filtration unless McrC is included. Together, the results show that although the tetradecameric $McrB_L$ complex can form in the absence of McrC, it is much more stable when McrC is present; note the absence of an ~400 kDa peak in the STEM histogram from $McrB_LC$ (Figure 3F). In agreement with this, the ratios between heptamer and tetradecamer varied between experiments; in one STEM experiment with $McrB_L$, only a minimal amount of the tetradecamer was observed (data not shown).

In gel filtration experiments, an intermediate with a mass between that of a monomer and a dimer (52 kDa for $McrB_S$ and 78 kDa for $McrB_L$) was observed for both $McrB_S$ and $McrB_L$ in the presence of GTP or GDP. These masses are below the range of STEM mass measurements at the recording doses employed. Since SDS–PAGE followed by silver staining did not reveal any additional proteins (data not shown), these species appear to be true assembly intermediates, possibly dimers, which, due to their non-ideal shape, elute with an apparent low relative molecular mass.

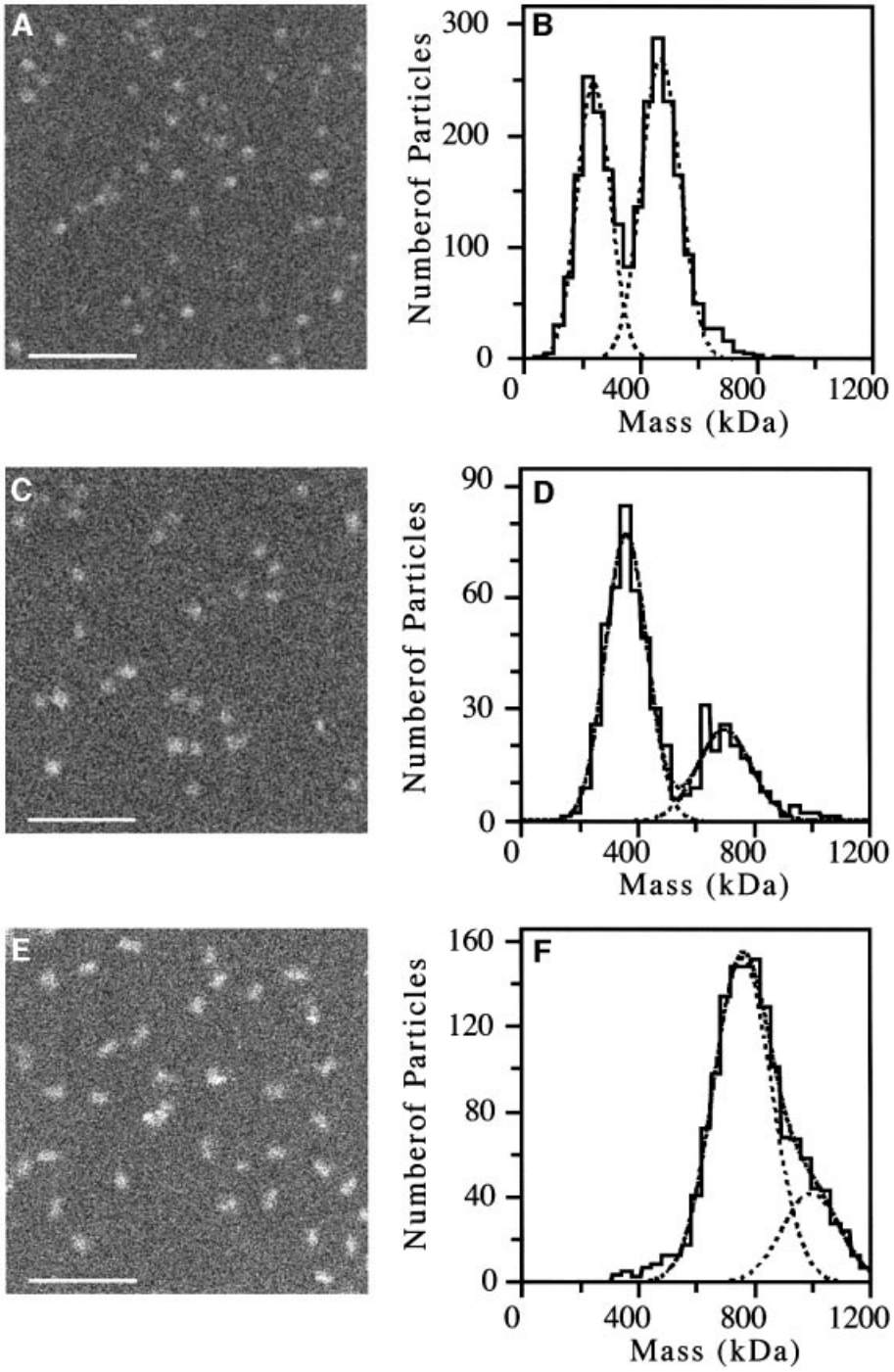

Fig. 3. STEM mass measurements. (**A**) Image of unstained $McrB_S$ particles. (**B**) Histogram showing the masses of the 2415 selected $McrB_S$ particles. The Gaussian curves fitted indicate two peaks with masses of 239 (± 57) and 468 (± 66) kDa. (**C**) Image of unstained $McrB_L$ particles. (**D**) Histogram showing the masses of the 572 selected $McrB_L$ particles. The Gaussian curves fitted indicate two peaks with masses of 361 (± 71) and 698 (± 93) kDa. (**E**) Image of unstained $McrB_LC$ particles. (**F**) Histogram showing the masses of the 1518 selected $McrB_LC$ particles. The Gaussian curves fitted indicate a main peak with a mass of 759 (± 100) kDa. An additional smaller peak with a mass of 994 (± 100) kDa was obtained. Correction has been made for beam-induced mass loss. Scale bars, 100 nm.

The oligomeric ring structures formed by $McrB_L$ and $McrB_S$ are reminiscent of those formed by hexameric helicases such as T7 gp4 (Patel and Hingorani, 1993), RuvB (Stasiak *et al*., 1994), DnaB (Reha-Krantz and Hurwitz, 1978), the SV40 T antigen (Mastrangelo *et al*., 1989) and the heptameric Rad52 (Stasiak *et al*., 2000). Like the eukaryotic SV40 T antigen, T7 gp4 and DnaB, which form hexameric complexes upon incubation with Mg^{2+} and nucleotide cofactor, oligomerization of $McrB_L$ and $McrB_S$ is dependent on the nucleotide cofactor. Assembly did not require GTP hydrolysis since both GDP and the non-hydrolyzable analog GTP-γ-S supported oligomerization. The N-terminal methylation-specific DNA-binding domain of McrBL targets the endonuclease

Table III. Masses (kDa) of McrBC complexes determined by scanning transmission electron microscopy

	No. of particles		Mass		SD		SE	
	Peak 1	Peak 2	Peak 1	Peak 2	Peak 1	Peak 2	Peak 1	Peak 2
$McrB_S$	~1053	~1318	239	468	57	66	2	2
$McrB_L$	402	166	361	698	71	93	4	7
$McrB_LC$	~1162	~265	759	994	100	100	3	6

The number of particles in each peak was estimated by measuring up to and away from curve crossover. The standard deviation (SD) as well as the standard error (SE) for each mass measurement is indicated.

Table IV. Stoichiometry of the McrBC endonuclease

	Monomer kDa	Peak 1 kDa	Ratio	Peak 2 kDa	Ratio
$McrB_S$	34.6	239	7.0	468	13.7
$McrB_L$	53.1	361	6.8	698	13.1
$McrB_LC$	–	759	$14B_L$ + 1(2)C	994	?

The ratio of subunits in each complex was obtained by dividing the measured mass of each complex by the calculated molecular weight for each subunit.

to assemble on the DNA. It remains unclear whether the DNA-binding domain resides in the channel region or on the exterior of the complex, as suggested at first glance by the additional protrusions exhibited by the McrBL oligomers (Figure 2B).

$McrB_L$ can bind to DNA in the absence of GTP-γ-S with an ~7-fold lower affinity than in its presence (Stewart *et al*., 2000). Therefore, it seems that G nucleotide-induced ring formation is not a prerequisite for DNA binding. The DNase I footprint of $McrB_L$ in the absence or presence of GTP-γ-S is identical, covering 16–18 bp around the methylated recognition site (Stewart *et al*., 2000). This indicates that either the $McrB_L$ monomer protects the same amount of DNA as the oligomer or that the DNA substrate induces $McrB_L$ oligomerization. Such DNA-induced oligomerization has been observed, for example, in the case of the hexameric E1 helicase (Fouts *et al*., 1999).

The location and exact stoichiometry of McrC in the McrBC endonuclease are still unclear. McrC interacts with the $McrB_L$–DNA complex as monitored by gel shift experiments (Stewart *et al*., 2000). According to DNase I footprint experiments in the presence of GTP-γ-S, McrC does not interact with the DNA (Stewart *et al*., 2000). The STEM data show that although the $McrB_L$ tetradecameric species is stabilized by McrC binding, both McrB subunits can form tetradecameric complexes in the absence of McrC (Figure 3). In addition, the mass measurements indicate the presence of up to two McrC proteins. Therefore, in our model for the assembly of the McrBC endonuclease, we tentatively place McrC outside of the two assembled heptameric rings (Figure 4).

$McrB_L$ and $McrB_S$ both have a weak intrinsic GTPase activity that is stimulated by McrC (data not shown; Pieper *et al*., 1997; Panne *et al*., 1999). In the case of $McrB_L$ (but not $McrB_S$) this McrC-stimulated GTPase activity is stimulated moderately by substrate DNA (Panne *et al*., 1999). DNA cleavage is dependent on GTP hydrolysis and is strongly inhibited by GTP-γ-S (data not shown; Sutherland *et al*., 1992). DNA cleavage requires the presence of two suitably modified recognition elements separated by 40–3000 bp in the DNA substrate (Sutherland *et al*., 1992; Stewart and Raleigh, 1998; Panne *et al*., 1999). Recent data support the model that GTP hydrolysis fuels DNA translocation by the endonuclease (Panne *et al*., 1999). DNA translocation is accomplished while the enzyme remains bound to the recognition sequence. Once translocation is stalled, by collision with either a second

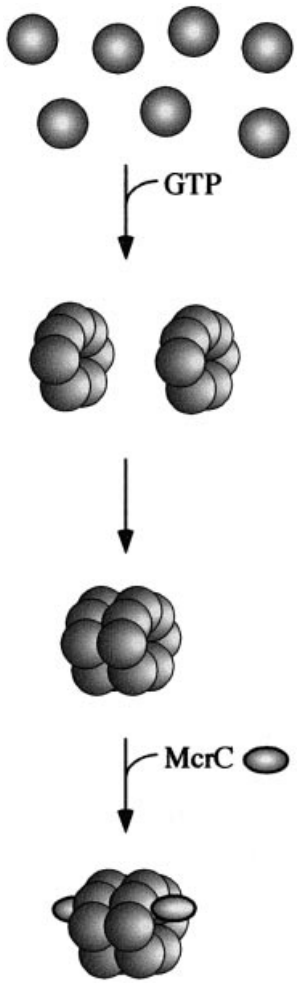

Fig. 4. Model for the assembly of the McrBC endonuclease complex. $McrB_L$ or $McrB_S$ assemble into heptameric rings in the presence of GTP or GDP. These rings can spontaneously dimerize into a tetradecamer. McrC binding stabilizes the tetradecameric form of the endonuclease.

translocating complex or a non-specific physical block, the enzyme cleaves the DNA in a region ~30 bp away from its recognition site (Panne *et al*., 1999). The ring structure of $McrB_L$ may link the endonuclease topologically to the DNA and thereby ensure processive translocation of the DNA along the nuclease. The fact that two recognition sites are normally required for DNA cleavage suggests that two complexes, each assembled on a single recognition site, collaborate in DNA cleavage (Sutherland *et al*., 1992;

Stewart and Raleigh, 1998; Panne *et al*., 1999). It is possible that a heptameric $McrB_L$ complex assembles on a single recognition site and that McrC binding then stimulates GTP hydrolysis and DNA translocation. Once two such complexes are brought into proximity, they engage to form the tetradecameric $McrB_LC$ cleavage complex. However, since it has been demonstrated that a single recognition site can be sufficient for assembly of a cleavage-competent complex (Panne *et al*., 1999) and because the tetradecameric complex forms in the absence of DNA, further experiments are required to reveal the stoichiometry of the enzyme complex on DNA.

The McrBC endonuclease is unique in several respects: it is the only endonuclease among the large and functionally divergent AAA+ family of proteins and it is the only restriction endonuclease with a ring-like structure. It is quite possible that the AAA+ proteins not only share sequence and structural similarities but that there are mechanistic similarities underlying their diverse biochemical functions. It has been suggested that the regulatory 19S cap complex of the eukaryotic 26S proteasome is involved in the unfolding and translocation of the substrate protein into the proteolytic core (Braun *et al*., 1999). Similarly, the role of the regulatory subunit ClpA in proteolysis by ClpAP is that of substrate unfolding and translocation into the proteolytic core of ClpP (Hoskins *et al*., 1998). Among the DNA-binding proteins of the AAA+ family, RuvB as well as DnaB and McrBC require DNA translocation at one stage of their reaction mechanism. The translocation of DNA on the one hand and that of substrate protein on the other may provide an unexpected link between these unrelated transport processes and reveal a common function for the AAA+ domain.

Materials and methods

Gel filtration

Gel filtration was carried out at 10°C on a Superdex 200 PC3.2/30 column using the Pharmacia SMART system. The column was equilibrated with buffer 1 [20 mM Tris–HCl pH 7.5 (21°C), 50 mM NaCl, 1 mM dithiothreitol (DTT)]. The same results were obtained using buffer 1 with 150 mM NaCl. The proteins were prepared as described previously (Panne *et al*., 1998) and stored at –20°C in storage buffer [10 mM Tris–HCl pH 7.5 (21°C), 200 mM NaCl, 0.1 mM Na_2EDTA, 1 mM DTT and 50% glycerol]. The sample was prepared by diluting the protein 10-fold into 100 µl of buffer 2 [10 mM Tris–HCl pH 7.9 (25°C), 10 mM $MgCl_2$, 50 mM NaCl, 1 mM DTT] with or without 1 mM nucleotide cofactor. The samples were incubated for 5 min at room temperature. For $McrB_S$, 50 µl of a 4.1 µM and for $McrB_L$, 50 µl of a 2.8 µM solution were injected into the column. For experiments with McrC, $McrB_L$ or $McrB_S$ was incubated as above and then McrC was added to a final concentration of 1.2 µM. The column was run at a flow rate of 40 µl/min. Absorbance was monitored at the wavelengths 215, 253 and 280 nm. Fractions of 80 µl were collected and the presence of protein was confirmed by SDS–PAGE and/or western blot analysis (data not shown). The column was calibrated under the same buffer conditions as above, using Blue 2000 dextran (Pharmacia) to determine the void volume $V_0 = 0.94$. The molecular weight standards were thyroglobulin (669 kDa) $V_e = 1.04$, ferritin (440 kDa) $V_e = 1.17$, aldolase (158 kDa) $V_e = 1.36$, bovine serum albumin (67 kDa) $V_e = 1.49$, ovalbumin (43 kDa) $V_e = 1.57$ and RNase A (13.7 kDa) $V_e = 1.83$. The K_{av} values were calculated using: $K_{av} = V_e - V_0/V_t - V_0$ and the total column volume V_t of 2.4 ml.

Scanning transmission electron microscopy and mass analysis

For both the $McrB_S$ and the $McrB_L$ experiments, 7.5 µl aliquots of 0.1 µM protein in buffer 2 with 1 mM GTP-γ-S were adsorbed for 1 min to glow-discharged thin carbon films. These spanned a thick fenestrated carbon layer covering 200 mesh/inch, gold-plated copper grids. For negative stain microscopy, the grids were blotted, washed with three drops of quartz double-distilled water, stained with 2% (w/v) uranyl formate for 20 s and air dried. For mass measurements, the grids were blotted and washed with five drops of quartz double-distilled water to remove buffer salts. A blotting step followed each wash. They were left unstained, frozen in liquid nitrogen and freeze-dried at –80°C at 5×10^{-8} Torr overnight in the microscope. $McrB_L$–McrC complexes were prepared by mixing 2 µM $McrB_L$, 1.2 µM McrC and 1 mM GTP-γ-S in buffer 2. The oligomers were purified by gel filtration as described above. The protein eluted in a single peak, was immediately supplemented with 1 mM GTP-γ-S and the sample was applied directly to the microscope grids, which were prepared for either negative stain microscopy or mass measurement as outlined above.

A Vacuum Generators STEM HB-5 interfaced to a modular computer system (Tietz Video and Image Processing Systems GmbH, D-8035 Gauting) was employed. Details of the instrument's calibration and use for mass measurement can be found in Engel (1978) and Müller *et al*. (1992). Series of 512 × 512 pixel, digital dark-field images were recorded from the unstained samples at an accelerating voltage of 80 kV. The nominal magnification was 200 000× and recording doses were in the range of 300 electrons/nm^2. In addition, repeated low dose scans were recorded from several grid regions of the samples to assess beam-induced mass loss.

The images recorded for mass measurement were evaluated using the program package IMPSYS as described (Müller *et al*., 1992). Accordingly, complexes were selected in circular boxes. The total scattering within the box was then calculated and the contribution arising from the carbon support film subtracted. The latter was determined from randomly selected regions on the same image. The resulting mass values were corrected for beam-induced mass loss, displayed in histograms and described by Gaussian curves. The mass loss relationship was determined experimentally from the behavior of both enzyme oligomers within the repeatedly imaged regions of the sample, by monitoring their mass as the total exposure dose increased up to 2000 electrons/nm^2 (Müller *et al*., 1992). The correction factors were 1.052 for the $McrB_S$ sample (recording dose 377 ± 49 electrons/nm^2), 1.043 for the $McrB_L$ sample (recording dose 315 ± 32 electrons/nm^2) and 1.035 for the $McrB_LC$ sample (recording dose 343 ± 21 electrons/nm^2). Series of 512 × 512 pixel, digital dark-field images were recorded at a nominal magnification of 500 000× from the corresponding negatively stained samples. In this case, the STEM was operated at an accelerating voltage of 100 kV and recording doses ranged from 4000 to 6000 and from 8000 to 10 000 electrons/nm^2.

Acknowledgements

We thank Fiona J.Stewart for providing us with purified McrC, and Elisabeth A.Raleigh for critical reading and suggestions for the improvement of the manuscript. This work was supported by the Swiss National Science Foundation grant number 31-42435.94 to A.E. and the M.E.Müller Foundation of Switzerland and grant number 31-46768.96 to T.A.B.

References

Arber,W. (1965) Host specificity of DNA produced by *Escherichia coli*: V. The role of methionine in the production of host specificity. *J. Mol. Biol.*, **11**, 247–256.

Beary,T.P., Braymer,H.D. and Achberger,E.C. (1997) Evidence of participation of McrBs in McrBC restriction in *Escherichia coli* K-12. *J. Bacteriol.*, **179**, 7768–7775.

Bertani,G. and Weigle,J.J. (1953) Host controlled variation in bacterial viruses. *J. Bacteriol.*, **65**, 113–121.

Bickle,T.A. and Krüger,D.H. (1993) The biology of DNA restriction. *Microbiol. Rev.*, **57**, 434–450.

Braun,B.C., Glickman,M., Kraft,R., Dahlmann,B., Kloetzel,P.M., Finley,D. and Schmidt,M. (1999) The base of the proteasome regulatory particle exhibits chaperone-like activity. *Nature Cell Biol.*, **1**, 221–226.

Confalonieri,F. and Duguet,M. (1995) A 200-amino acid ATPase module in search of a basic function. *BioEssays*, **17**, 639–650.

Dila,D., Sutherland,E., Moran,L., Slatko,B. and Raleigh,E.A. (1990) Genetic and sequence organization of the *mcrBC* locus of *Escherichia coli* K-12. *J. Bacteriol.*, **172**, 4888–4900.

Dussoix,D. and Arber,W. (1962) Host specificity of DNA produced by *Escherichia coli*: II. Control over acceptance of DNA from infecting phage λ. *J. Mol. Biol.*, **5**, 37–49.

Engel,A. (1978) Molecular weight determination by scanning transmission electron microscopy. *Ultramicroscopy*, **3**, 273–281.

Fouts,E.T., Yu,X., Egelman,E.H. and Botchan,M.R. (1999) Biochemical and electron microscopic image analysis of the hexameric E1 helicase. *J. Biol. Chem.*, **274**, 4447–4458.

Gast,F.U., Brinkmann,T., Pieper,U., Krüger,T., Noyer-Weidner,M. and Pingoud,A. (1997) The recognition of methylated DNA by the GTP-dependent restriction endonuclease McrBC resides in the N-terminal domain of McrB. *Biol. Chem.*, **378**, 975–982.

Hoskins,J.R., Pak,M., Maurizi,M.R. and Wickner,S. (1998) The role of the ClpA chaperone in proteolysis by ClpAP. *Proc. Natl Acad. Sci. USA*, **95**, 12135–12140.

Krüger,T., Grund,C., Wild,C. and Noyer-Weidner,M. (1992) Characterization of the *mcrBC* region of *Escherichia coli* K12 wild-type and mutant strains. *Gene*, **114**, 1–12.

Krüger,T., Wild,C. and Noyer-Weidner,M. (1995) McrB: a prokaryotic protein specifically recognizing DNA containing modified cytosine residues. *EMBO J.*, **14**, 2661–2669.

Luria,S.E. and Human,M.L. (1952) A nonhereditary, host-induced variation of bacterial viruses. *J. Bacteriol.*, **64**, 557–569.

Mastrangelo,I.A., Hough,P.V., Wall,J.S., Dodson,M., Dean,F.B. and Hurwitz,J. (1989) ATP-dependent assembly of double hexamers of SV40 T antigen at the viral origin of DNA replication. *Nature*, **338**, 658–662.

Müller,S.A., Goldie,K.N., Bürki,R., Häring,R. and Engel,A. (1992) Factors influencing the precision of quantitative scanning transmission electron microscopy. *Ultramicroscopy*, **46**, 317–334.

Neuwald,A.F., Aravind,L., Spouge,J.L. and Koonin,E.V. (1999) AAA$^+$: a class of chaperone-like ATPases associated with the assembly, operation and disassembly of protein complexes. *Genome Res.*, **9**, 27–43.

Pamnani,V., Tamura,T., Lupas,A., Peters,J., Cejka,Z., Ashraf,W. and Baumeister,W. (1997) Cloning, sequencing and expression of VAT, a CDC48/p97 ATPase homologue from the archaeon *Thermoplasma acidophilum*. *FEBS Lett.*, **404**, 263–268.

Panne,D., Raleigh,E.A. and Bickle,T.A. (1998) McrBs, a modulator peptide for McrBC activity. *EMBO J.*, **17**, 5477–5483.

Panne,D., Raleigh,E.A. and Bickle,T.A. (1999) The McrBC endonuclease translocates DNA in a reaction dependent on GTP hydrolysis. *J. Mol. Biol.*, **290**, 49–60.

Patel,S.S. and Hingorani,M.M. (1993) Oligomeric structure of bacteriophage T7 DNA primase/helicase proteins. *J. Biol. Chem.*, **268**, 10668–10675.

Patel,S. and Latterich,M. (1998) The AAA team: related ATPases with diverse functions. *Trends Cell Biol.*, **8**, 65–71.

Pieper,U., Brinkmann,T., Kruger,T., Noyer,W.M. and Pingoud,A. (1997) Characterization of the interaction between the restriction endonuclease McrBC from *E.coli* and its cofactor GTP. *J. Mol. Biol.*, **272**, 190–199.

Raleigh,E.A. (1992) Organization and function of the *mcrBC* genes of *Escherichia coli* K-12. *Mol. Microbiol.*, **6**, 1079–1086.

Raleigh,E.A. and Wilson,G. (1986) *Escherichia coli* K-12 restricts DNA containing 5-methylcytosine. *Proc. Natl Acad. Sci. USA*, **83**, 9070–9074.

Reha-Krantz,L.J. and Hurwitz,J. (1978) The *dnaB* gene product of *Escherichia coli*. I. Purification, homogeneity and physical properties. *J. Biol. Chem.*, **253**, 4043–4050.

Revel,H.R. (1983) DNA modification: glucosylation. In Mathews,C.K., Kutter,E.M., Mosig,G. and Berget,P. (eds), *Bacteriophage T4*. American Society for Microbiology, Washington, DC, pp. 156–165.

Roberts,R.J. and Macelis,D. (1993) The restriction enzymes. In Linn,S.M., Lloyd,R.S. and Roberts,R.J. (eds), *Nucleases*. Cold Spring Harbor Laboratory Press, Cold Spring Harbor, NY, pp. 439–444.

Rohrwild,M., Pfeifer,G., Santarius,U., Müller,S.A., Huang,H.C., Engel, A., Baumeister,W. and Goldberg,A.L. (1997) The ATP-dependent HslVU protease from *Escherichia coli* is a four-ring structure resembling the proteasome. *Nature Struct. Biol.*, **4**, 133–139.

Ross,T.K. and Braymer,H.D. (1987) Localization of a genetic region involved in McrB restriction by *Escherichia coli* K-12. *J. Bacteriol.*, **169**, 1757–1759.

Ross,T.K., Achberger,E.C. and Braymer,H.D. (1989a) Identification of a second polypeptide required for McrB restriction of 5-methylcytosine-containing DNA in *Escherichia coli* K-12. *Mol. Gen. Genet.*, **216**, 402–407.

Ross,T.K., Achberger,E.C. and Braymer,H.D. (1989b) Nucleotide sequence of the McrB region of *Escherichia coli* K-12 and evidence for two independent translational initiation sites at the *mcrB* locus. *J. Bacteriol.*, **171**, 1974–1981.

Stasiak,A., Tsaneva,I.R., West,S.C., Benson,C.J., Yu,X. and Egelman, E.H. (1994) The *Escherichia coli* RuvB branch migration protein forms double hexameric rings around DNA. *Proc. Natl Acad. Sci. USA*, **91**, 7618–7622.

Stasiak,A.Z., Larquet,E., Stasiak,A., Müller,S., Engel,A., Van Dyck,E., West,S.C. and Egelman,E.H. (2000) The human Rad52 protein exists as a heptameric ring. *Curr. Biol.*, **10**, 337–340.

Stewart,F.J. and Raleigh,E.A. (1998) Dependence of McrBC cleavage on distance between recognition elements. *Biol. Chem.*, **379**, 611–616.

Stewart,F.J., Panne,D., Bickle,T.A. and Raleigh,E.A. (2000) Methyl-specific DNA binding by McrBC, a modification-dependent restriction enzyme. *J. Mol. Biol.*, **298**, 611–622.

Sutherland,E., Coe,L. and Raleigh,E.A. (1992) McrBC: a multisubunit GTP-dependent restriction endonuclease. *J. Mol. Biol.*, **225**, 327–358.

Wolf,S., Nagy,I., Lupas,A., Pfeifer,G., Cejka,Z., Müller,S.A., Engel,A., De Mot,R. and Baumeister,W. (1998) Characterization of ARC, a divergent member of the AAA ATPase family from *Rhodococcus erythropolis*. *J. Mol. Biol.*, **277**, 13–25.

Received February 28, 2001; revised April 5, 2001; accepted April 23, 2001